



# Kinetic and mechanistic study of photocatalytic degradation of flame retardant Tris (1-chloro-2-propyl) phosphate (TCPP)



M. Antonopoulou<sup>a,b</sup>, P. Karagianni<sup>a</sup>, I.K. Konstantinou<sup>b,\*</sup>

<sup>a</sup> Department of Environmental and Natural Resources Management, University of Patras, 30100, Agrinio, Greece

<sup>b</sup> Department of Chemistry, University of Ioannina, 45110 Ioannina, Greece

## ARTICLE INFO

### Article history:

Received 11 October 2015

Received in revised form 11 March 2016

Accepted 16 March 2016

Available online 18 March 2016

### Keywords:

Flame retardants

TCPP

Photocatalysis

Scavengers

Transformation products

## ABSTRACT

In the present work, a comprehensive study on the application of TiO<sub>2</sub> photocatalysis for the removal of the flame retardant tris (1-chloro-2-propyl) phosphate (TCPP) from both ultrapure water (UW) and real wastewater (WW) is presented. All the photocatalytic experiments were conducted using environmental relevant concentrations of TCPP, inherent pH and simulated solar irradiation with the view to simulate real environmental conditions. Degradation followed apparent first-order kinetics with rate constants varying from  $k_{app} = 14.2 \times 10^{-2} \text{ min}^{-1}$  to  $k_{app} = 1.41 \times 10^{-2} \text{ min}^{-1}$  for initial TCPP concentrations in the range of 25–500  $\mu\text{g L}^{-1}$  while mineralization was accomplished in prolonged irradiation times as monitored by the release of chlorine and phosphate ions. Scavenging studies were carried out in UW, indicating that photogenerated HO<sup>•</sup> in the catalyst surface are the main species participating in the photocatalytic mechanism. Experiments using secondary treated wastewater showed a significant retardation of TCPP photocatalytic degradation mainly due to scavenging effects and competitive adsorption of aromatic and phenolic compounds and inorganic ions, such as HCO<sub>3</sub><sup>−</sup>, contained in the wastewater matrix. The transformation products were elucidated by UPLC-TOF-MS instrumentation and hydroxylation, oxidation, dechlorination and dealkylation have been identified as the principal photocatalytic transformation routes before complete mineralization. Toxicity assays in UW and WW were also conducted using *Vibrio fischeri* as tested organism showing a progressive toxicity decrease along the treatment till low values. Measurements showed a higher initial toxicity and a slower decrease in WW that is attributed to the more complex matrix regarding chemical pollutants and their transformation products formed during the treatment as well as scavenging effects.

© 2016 Elsevier B.V. All rights reserved.

## 1. Introduction

The efficiency of heterogeneous photocatalysis for the removal of a great number of organic contaminants from aqueous phase is well-documented in the literature [1–3]. An increasing number of scientific works are focused on the photocatalytic removal of aquatic pollutants such as personal care products, pharmaceuticals, pesticides, taste and odor compounds, veterinary products and food additives, among others, demonstrating promising results [1–7]. The efficiency of the process has been associated with the generation of various oxidizing and reductive species when the photocatalyst is illuminated with energy greater than its band gap [1–3,7]. Although heterogeneous photocatalysis has become a field of extensive research during the last decades, the photocatalytic

removal of aquatic pollutants belonging to the category of flame retardants is scarce.

Flame retardants (FRs) constitute a class of emerging contaminants as their heavy use in consumer and building products, has led to their presence in air, water and sediments at various concentration levels [8–12]. FRs are considered to be environmentally persistent and exert ecotoxicological effects at relatively low concentrations [9,10,12]. In recognition of their adverse effects on aquatic ecosystem and human health, various FRs are under evaluation in the framework of Toxic Substances Control Act from U.S. Environmental Protection Agency (USEPA) [9].

Among FRs, we have focused on the aliphatic halogenated phosphate ester, tris (1-chloro-2-propyl) phosphate (TCPP), a compound included in the European Commission fourth priority list [10]. Due its heavy production and major application, TCPP has also been categorized as an EU high production volume (HPV) chemical [10]. Recent studies have reported the occurrence of TCPP in natural water bodies and effluents as a result of incomplete removal by

\* Corresponding author.

E-mail address: [iokonst@cc.uoi.gr](mailto:iokonst@cc.uoi.gr) (I.K. Konstantinou).

conventional wastewater treatment plants (WWTPs) [10,12]. TCP P has been detected in effluent and surface water samples at concentrations as high as  $24 \mu\text{g L}^{-1}$  and  $200 \text{ ng L}^{-1}$ , respectively [10,12].

The main focus of the present work is to provide novel knowledge in relation to the applicability of heterogeneous  $\text{TiO}_2$  photocatalysis to remove TCP P, a representative flame retardant pollutant, from water matrices that is studied for the first time. For this purpose, the photocatalytic transformation of TCP P was investigated using concentrations similar to those detected in real effluents and two different aqueous matrices, ultrapure water (UW) and municipal wastewater secondary treatment effluent (WW). More specifically, the photocatalytic transformation of TCP P in UW and WW, in terms of pollutant abatement and mineralization and the effect of the matrix on the transformation process were evaluated. The contribution of oxidative and reductive species generated during the process was studied in detail using various well-established scavengers. Emphasis was also placed on the identification of the transformation products using ultra pressure liquid chromatography coupled to time-of-flight mass spectrometry (UPLC-TOF-MS). Finally, the study focused also on the integrated evaluation of the treatment process by assessing the evolution of ecotoxicity during the treatment.

## 2. Experimental

### 2.1. Chemicals

TCP P (mixtures of isomers), analytical standard was obtained by Sigma-Aldrich (USA).  $\text{TiO}_2$  P25 (Evonik, Germany; particle size 20–30 nm; crystal structure, 80% anatase and 20% rutile; surface area,  $56 \text{ m}^2 \text{ g}^{-1}$ , zero point of charge  $\approx 6.3\text{--}6.8$ ) was employed as the semiconductor catalyst in the photocatalytic experiments. All reagents used (sodium azide ( $\text{NaN}_3$ ), KI, *p*-benzoquinone (BQ), NaF,  $\text{K}_2\text{Cr}_2\text{O}_7$  and Folin Ciocalteu) were obtained from Sigma-Aldrich. LC-MS-grade solvents (acetonitrile, isopropanol, methanol and water) were supplied by Merck and used for UPLC-TOF-MS analyses. In order to remove the  $\text{TiO}_2$  particles of the solution samples during the experiments, HA  $0.45 \mu\text{m}$  filters were supplied by Millipore (Bedford, USA). Oasis HLB (divinylbenzene/*N*-vinylpyrrolidone copolymer) cartridges (60 mg, 3 mL) from Waters (Mildford, MA, USA) were used for the extraction of water samples and the identification of transformation products. TCP P solutions were prepared both in ultrapure water (Milli-Q) and secondary (conventional activated sludge) treated municipal wastewater samples (WW). Samples of WW were collected directly from the treatment plant of Patras University, West Greece. After collection, the samples were transferred to the laboratory immediately and filtered to remove particulate matter. Mean values of physicochemical parameters of the WW were: pH  $7.85 \pm 0.04$ ; conductivity  $= 310.51 \pm 25.3 \mu\text{S cm}^{-1}$ ; Total suspended solids  $= 1.07 \pm 0.013 \text{ mg L}^{-1}$ ; Chemical oxygen demand  $= 18.9 \pm 1.82 \text{ mg L}^{-1}$ ; Total organic carbon  $= 6.2 \pm 0.18 \text{ mg L}^{-1}$ ; TPh  $= 1.03 \pm 0.015 \text{ mg L}^{-1}$ ;  $\text{PO}_4^{3-} = 1.85 \pm 0.017 \text{ mg L}^{-1}$ ;  $\text{SO}_4^{2-} = 30 \pm 0.96 \text{ mg L}^{-1}$ ;  $\text{NO}_3^- = 20.5 \pm 0.48 \text{ mg L}^{-1}$ .

### 2.2. Photocatalytic experiments

Photocatalytic experiments were carried out in a solar simulator Suntest XLS+ apparatus (Atlas, Germany) equipped with a 2.2 kWatt xenon lamp jacketed and special glass filters cutting the irradiation with wavelengths below 290 nm. In each experiment 250 mL of aqueous solutions with the desired concentration of TCP P and the appropriate amount of catalyst ( $50 \text{ mg L}^{-1}$ ) were loaded in Pyrex glass UV-reactor at ambient conditions (temperature  $= 23^\circ\text{C}$  and pH 6.5) under continuous stirring. The catalyst loading level

( $50 \text{ mg L}^{-1}$ ) was selected based on the low environmental relevant concentration levels used in the irradiation experiments in order to not obtain very fast kinetics and to facilitate the study on the degradation kinetics, mechanisms and identification of transformation products. Prior to exposure to simulated solar irradiation, the suspension was magnetically stirred for 30 min in the dark to ensure adsorption equilibrium of TCP P onto the  $\text{TiO}_2$  surface. The radiation intensity was fixed at  $250 \text{ W m}^{-2}$  for all experiments and the incident irradiance dose for 10 min of irradiation was  $150 \text{ kJ m}^{-2}$  as provided by an internal radiometer of Suntest instrument. Samples of about 2 mL were periodically withdrawn from the reactor and filtered for further analysis.

### 2.3. Analytical determinations

TCP P quantification and identification of transformation products was performed by means of UPLC coupled to a time of flight mass spectrometry (UPLC-TOF-MS) system in positive ionization mode. Samples (20 mL) were pre-concentrated by means of solid phase extraction (SPE) as reported in our previous study to a final volume of 0.2 mL [5]. The UPLC-TOF-MS system consisted of an Ultra-High Performance LC pump (Dionex Ultimate 3000, Thermo) equipped with a C18 Acclaim<sup>TM</sup> RSLC 120 column, 100 mm  $\times$  2.1 mm, 2.2  $\mu\text{m}$  particle size (Thermo Fisher Scientific, San Jose, USA), thermostated at  $30^\circ\text{C}$  and a microTOF Focus II – time of flight mass spectrometer (Brüker Daltonics, Germany). A and B mobile phases were methanol and water with 5 mM ammonium formate respectively, at a flow rate of  $0.4 \text{ mL min}^{-1}$ . The following program was adopted: 1% A/99% B at 0 min to 99% A/1% B in 10 min and back to the initial ratio in 13 min. The injection volume was 10  $\mu\text{L}$ . The TOF mass analyzer with an electrospray interface was operated under the following conditions: dry gas flow rate  $8 \text{ L min}^{-1}$  (nitrogen), nebulizer pressure 2.4 bar, capillary voltage at 4500 V, end plate offset at 500 V, hexapole RF 100.0 Vpp, dry temperature at  $200^\circ\text{C}$  using otof control software. The mass accuracy ( $\pm 5 \text{ ppm}$ ) of the TOF mass analyzer was ensured by an externally calibration using sodium formate, in the scan range  $m/z$  50–1000, prior to analysis. Under the adopted chromatographic conditions, TCP P retention time was 8.1 min. The limit of detection (LOD) and limit of quantitation (LOQ) was 50 and  $165 \text{ ng L}^{-1}$ , respectively.

Aromatic compounds content in WW sample was evaluated by means of the absorbance at 254 nm that was monitored using a UV-vis spectrophotometer (Hitachi, U-2000). The total phenols were determined by the Folin-Ciocalteu method. The phenolic content (TPh) was expressed as  $\text{mg L}^{-1}$  of equivalent phenol, using a calibration curve based on standard solutions of phenol.  $\text{Cl}^-$  and  $\text{PO}_4^{3-}$  ions, released during the oxidation of TCP P, were determined by a Dionex ICS-1500 Ion Chromatography system incorporated with an ASRS Ultra II suppressor. Analysis was performed on an Ion-Pac AS9-HC using an aqueous sodium carbonate (9 mM) solution as mobile phase was at a flow rate of  $1 \text{ mL min}^{-1}$ .

### 2.4. Scavenging experiments

The role of  $\text{HO}^\bullet$ ,  $\text{h}^+$ ,  $\text{e}^-_{\text{aq}}$  and  $\text{O}_2^{\bullet-}$  in the degradation mechanism was assessed by the addition of  $1 \times 10^{-3} \text{ M}$  isopropanol (i-PrOH),  $1 \times 10^{-3} \text{ M}$   $\text{I}^-$ ,  $50 \times 10^{-3} \mu\text{M}$   $\text{K}_2\text{Cr}_2\text{O}_7$ ,  $1 \times 10^{-3} \text{ M}$  *p*-BQ and  $1 \times 10^{-3} \text{ M}$   $\text{N}_3^-$ , respectively. Photocatalytic experiments with the addition of  $1 \times 10^{-3} \text{ M}$  methanol as well as using MeCN as reaction media were also conducted for discrimination between the oxidation by  $\text{HO}^\bullet$  and  $\text{h}^+$ . To wash  $\text{HO}^\bullet_{\text{ads}}$  into solution as bulk  $\text{HO}^\bullet_{\text{bulk}}$ , NaF at  $0.1 \times 10^{-3} \text{ mM}$  was used. Finally, aqueous solutions of TCP P degassed with high-purity  $\text{N}_2$  were also subjected to photocatalytic treatment [13,14].

### 2.5. Toxicity evolution during photocatalytic treatment

The evolution of toxicity during the photocatalytic treatment was assessed by the well-described in the literature *Vibrio fischeri* assay, using a Microtox® Model 500 Toxicity Analyzer (Azur Environmental) [14,15]. The inhibition of luminescence was recorded after 5, 15, 30, 60 and 90 min of incubation at 15 °C.

## 3. Results and discussion

### 3.1. Preliminary experiments

Previous to the photocatalytic experiments, preliminary photolysis, adsorption and hydrolysis experiments were performed in both ultrapure and WW with a TCP P concentration of 25 µg L<sup>-1</sup>. As shown in Fig. 1S (Supporting information), no significant removal of the investigated flame retardant in the dark and under simulated solar irradiation, in both matrices was observed. More specifically, the direct photolysis showed that only 4% and 7% of TCP P was removed after 240 min of simulated solar illumination in ultrapure and WW, respectively. About 9% of the initial TCP P concentration was adsorbed onto the catalyst in the dark, after 30 min of continuous stirring, in both matrices. Similarly, hydrolysis experiments showed negligible transformation of the compound (data not shown).

### 3.2. Heterogeneous photocatalysis with TiO<sub>2</sub>

Degradation kinetics of TCP P by TiO<sub>2</sub> heterogeneous photocatalysis at various environmental relevant initial concentrations ( $C_0 = 25 - 500 \mu\text{g L}^{-1}$ ) in ultrapure water is depicted in Fig. 1a. TCP P was completely degraded in ultrapure water after 30–180 min of photocatalytic treatment depending on the initial concentration of the target compound. As shown in Fig. 1a, increasing initial TCP P concentration has a negative effect on the first order degradation reaction rates. With an increase in TCP P concentration, the ratio of available oxidative species ( $\text{HO}^\bullet$  and  $h^+$ ) to the substrate concentration decreases, leading to extension of degradation time. Moreover, competitive action for the oxidative species between target compound and generated TP s could take place as a consequence of increased intermediates formation at higher substrate concentrations [16,17]. The degradation kinetics of TCP P at the same experimental conditions as a function of the irradiation dose ( $\text{kJ m}^{-2}$ ) measured by Suntest apparatus are also given in Fig. 2S (Supporting information).

Chloride ( $\text{Cl}^-$ ) and phosphates ( $\text{PO}_4^{3-}$ ) ions were monitored by IC during the photocatalytic treatment carried out using 250 µg L<sup>-1</sup> as initial concentration in ultrapure water and the results are depicted in Fig. 1b. Similar investigation in WW photocatalytic experiments was not possible to be conducted due to the interferences provoked by its chemical composition. As progressive mineralization takes place, the heteroatoms present in TCP P molecule are released in the form of  $\text{Cl}^-$  and  $\text{PO}_4^{3-}$  ions.  $\text{Cl}^-$  and  $\text{PO}_4^{3-}$  reached after 300 min of irradiation about 95.6% and 64.5% of the expected stoichiometric chlorine and phosphorous amount, respectively. At the same time period the pH of the suspension was evolved from 6.3 to 5.4. The lack of phosphorous stoichiometric recovery indicated: (a) the presence of P-containing compounds, at the end of the process prior to TCP P complete mineralization to  $\text{CO}_2$  and  $\text{H}_2\text{O}$ ; and (b) the adsorption of phosphates ions in TiO<sub>2</sub> surface as reviewed for organophosphate pesticides elsewhere [1]. An adsorption experiment using 150 µg L<sup>-1</sup> of phosphate ions (close to the concentration theoretically released from TCP P mineralization) and 50 mg L<sup>-1</sup> of catalyst showed about 30% of phosphate adsorption thus taking into account this percentage the stoichiometric

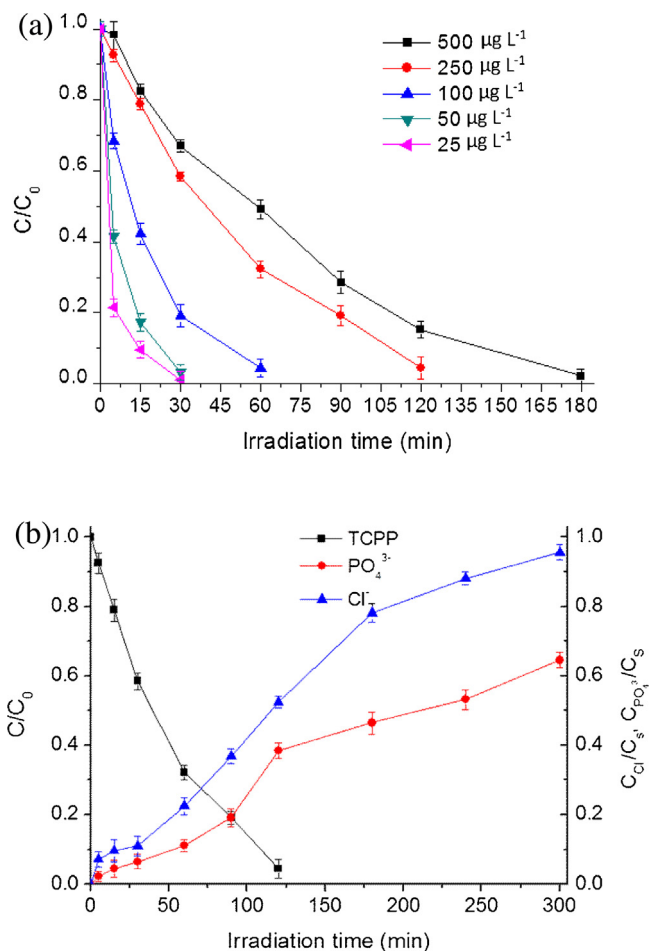


**Fig. 1.** (a) Degradation kinetics of TCP P ( $C_0 = 25 - 500 \mu\text{g L}^{-1}$ ) in aqueous TiO<sub>2</sub> suspensions (50 mg L<sup>-1</sup>) under simulated solar light ( $I = 250 \text{ W m}^{-2}$ ) in UW, (b) Evolution of  $\text{Cl}^-$  and  $\text{PO}_4^{3-}$  ions ( $[\text{TCP P}] = 250 \mu\text{g L}^{-1}$ ,  $[\text{TiO}_2] = 50 \text{ mg L}^{-1}$ ,  $I = 250 \text{ W m}^{-2}$ ) in UW.

amount is closely reached. A slower release and lower amounts of  $\text{PO}_4^{3-}$  ions at the end of the process and a rapid release of  $\text{Cl}^-$  has also been reported by other research groups which investigated the photocatalytic degradation of aliphatic organophosphorus compounds such as dichlorvos [18,19].

To estimate the effect of water matrix on the photocatalytic efficiency, real secondary treated WW samples were spiked with 25 µg L<sup>-1</sup> TCP P. This concentration was selected in order to simulate the highest concentration that has been detected in wastewater effluents. As clearly seen in Fig. 2, a significant inhibition in the degradation of TCP P was observed in WW and about 32% removal was achieved after 240 min. Similar results have been reported by other researchers [20–22], showing that the photocatalytic degradation of pharmaceutical and other organic pollutants was strongly hindered in wastewater matrices. The degradation kinetics of TCP P in WW matrix as a function of the irradiation dose ( $\text{kJ m}^{-2}$ ) measured by Suntest apparatus is also given in Fig. 3S (Supporting information). The observed results may be explained by the presence of (i) organic carbon that can react with hydroxyl radical ( $\text{HO}^\bullet$  scavenging reaction rate constants,  $k_{\text{HO}^\bullet}$ , with natural organic matter is reported in the range  $1.0 - 2.0 \times 10^8 \text{ M}^{-1} \text{ s}^{-1}$ ) [23] and (ii) various species such as inorganic ions that can quench reactive species generated during heterogeneous photocatalysis leading to less reactive or non-reactive radical species [24,25] or adsorbed into the catalyst surface covering reactive sites.

Considering, the aliphatic structure of TCP P and the documented in the literature preference of  $\text{HO}^\bullet$  radicals attack on the aro-

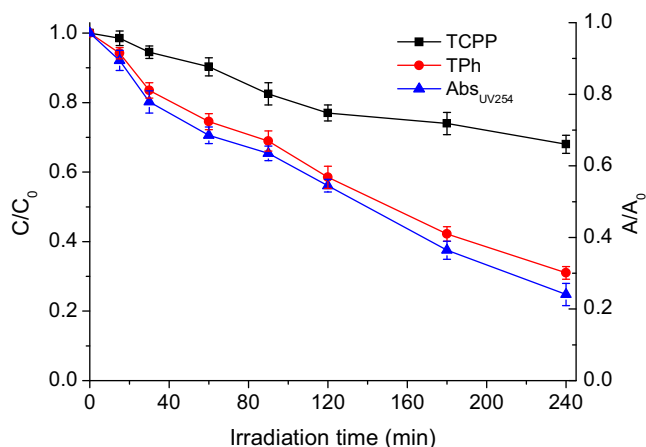


**Fig. 2.** Degradation kinetics of TCP ( $C_0 = 25 \mu\text{g L}^{-1}$ ) and TPh and evolution of absorbance at 254 nm, in aqueous  $\text{TiO}_2$  suspensions ( $50 \text{ mg L}^{-1}$ ) under simulated solar light ( $I = 250 \text{ W m}^{-2}$ ) in WW.

matic ring in comparison with the attack on the alkyl chain [26], the removal of total phenolic compounds as well as the aromatic organic content of wastewater was followed in concomitance with TCP abatement. Their removal during the photocatalytic treatment is illustrated in Fig. 2. About 70% of total phenols removal was recorded after 240 min of photocatalytic treatment and after that time, levels below the detection limits were reached. The relative fast kinetics are consistent with the reported high rate constants ( $10^9 - 10^{10} \text{ LM}^{-1} \text{ s}^{-1}$ ) [27] of  $\text{HO}^\bullet$  reaction with phenolics. The absorbance at 254 nm appeared to decrease progressively, reaching a reduction of 75% at the end of the process. The significant reduction of aromatic and phenolic organic content compared to TCP removal during the photocatalytic treatment can explain partially the significant inhibitory effect of water constituents on TCP removal as well as the importance of pollutants chemical structure for the potential  $\text{HO}^\bullet$  radicals attack, in real matrices. Finally, given the above mentioned  $k_{\text{OH}}$  rate constants for NOM and phenolics that are similar or higher compared to the  $k_{\text{OH}}$  reaction constant for TCP ( $1.98 \times 10^8 \text{ M}^{-1} \text{ s}^{-1}$ , [28]) and the much higher concentration of dissolved organic carbon compared to the concentration of TCP, the significant inhibition in TCP photocatalytic degradation in wastewaters is fully justified.

In addition, inorganic anions, such as phosphate, sulphate, nitrate and chloride ions, contained in the wastewater, have been reported to retard the photocatalytic of organic pollutants [4,26,29–31]. Retardation effects are related with the reaction between positive  $\text{h}^+$  and  $\text{HO}^\bullet$  with anions, that behave as  $\text{h}^+$  and  $\text{HO}^\bullet$  scavengers. High rate constants for reaction with hydroxyl radicals were reported for chloride ions ( $k = 4.3 \times 10^9 \text{ LM}^{-1} \text{ s}^{-1}$ ), sulfate ions ( $k = 1.0 \times 10^{10} \text{ LM}^{-1} \text{ s}^{-1}$ ) and carbonates, bicarbonates ions ( $k = 3.8 \times 10^8$  and  $1.0 \times 10^7$ , respectively), lower for phosphate ( $k < 1.0 \times 10^7 \text{ LM}^{-1} \text{ s}^{-1}$ ) and dihydrogen phosphate ( $k < 10^6 \text{ LM}^{-1} \text{ s}^{-1}$ ) anions while  $\text{NO}_3^-$  can be considered as poor  $\text{HO}^\bullet$  scavenger ( $k < 1.0 \times 10^5 \text{ LM}^{-1} \text{ s}^{-1}$ ) [27]. Taking into account the reaction rate constant of  $\text{HO}^\bullet$  towards TCP molecule ( $1.98 \times 10^8 \text{ LM}^{-1} \text{ s}^{-1}$ ) and the wastewater media physicochemical characteristics the most probable quenching effect are expected for sulphate and bicarbonate ions. The resulting inorganic radicals such as  $\text{Cl}^\bullet$  (2.47 V)  $\text{NO}_3^\bullet$  (2.3–2.5 V),  $\text{SO}_4^{\bullet-}$  (2.5–3.1 V) and  $\text{CO}_3^{\bullet-}$  (1.6 V) exhibit in most cases a lower oxidation potential than the main oxidant species participating in the process,  $\text{h}^+$  (2.6 V) and  $\text{HO}^\bullet$  (2.6–2.8 V), although in some cases (e.g.  $\text{SO}_4^{\bullet-}$ ) present also a higher selectivity. In addition, some inorganic radicals, e.g.  $\text{CO}_3^{\bullet-}$ , reacts more slowly than  $\text{HO}^\bullet$  with most organic substrates [32,33].

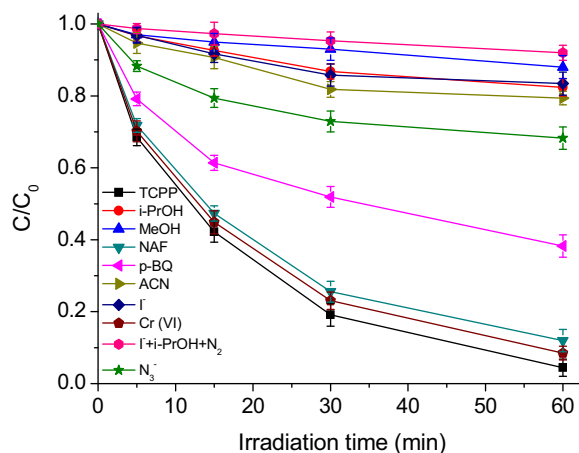


**Fig. 3.** Degradation kinetics of TCP ( $C_0 = 100 \mu\text{g L}^{-1}$ ) in the presence of scavengers in aqueous  $\text{TiO}_2$  suspensions ( $50 \text{ mg L}^{-1}$ ) under simulated solar light ( $I = 250 \text{ W m}^{-2}$ ).

Besides radical scavenging, the competitive adsorption of inorganic anions is considered as an additional potential mechanism of inhibition, covering the available reactive sites of the photocatalyst for reaction with the organic substrate and forming a surrounding layer [22,34]. The competition for the catalyst surface is influenced by the ionization state of titania thus, a more pronounced negative effect of inorganic anions on the photocatalytic degradation of organic substrates was usually recorded for  $\text{pH} < \text{pH}_{\text{PZC}}$  of the photocatalyst, as in the present study, since negatively charged ions are adsorbed in a greater extent in the positively charged titania surface. Finally, some anions (e.g.  $\text{NO}_3^-$ ,  $\text{SO}_4^{2-}$ ) may raise the turbidity of the solution, which could cause the screening of UV radiation when applying photocatalytic treatments [35]. For example, nitrates absorb light in the range of 300–310 nm and in 360 nm consequently high nitrate concentrations can limit the effectiveness of the photocatalytic process due to “inner filter” effect that lead to the decrease of the semiconductor photoexcitation. However, taking into account the low molar absorption coefficients at 360 nm ( $\lambda = 22.5 \text{ M}^{-1} \text{ cm}^{-1}$ ) and 310 nm ( $\lambda = 7.4 \text{ M}^{-1} \text{ cm}^{-1}$ ) and the concentration of nitrates in the wastewater, the inner filter effect due to  $\text{NO}_3^-$  could be neglected. On the contrary, nitrates could participate in photo-reactions that generate  $\text{HO}^\bullet$  radicals. However, the production of  $\text{HO}^\bullet$  radicals is expected to have a significant contribution in the photocatalytic degradation of organic substrates only during irradiation from a short UVC ( $\lambda > 200 \text{ nm}$ ) source [36] that is not the case in the present study.

In conclusion, the inhibiting effect of inorganic ions is affected by the interplay of factors such as  $\text{HO}^\bullet$  quenching rate constants and reaction rate constants of the resulting inorganic radicals towards the organic substrate, the competitive adsorption towards catalyst surface and the concentration ratio of ions versus the organic substrate or other organic matter present in the reaction media.

### 3.3. Contribution of reactive species in the degradation mechanism-Scavenging study

The contribution of various oxidizing and reductive species generated during the process was estimated through scavenging experiments in ultrapure water, by adding excess of well-documented in the literature quenching reagents. Fig. 3 displays the degradation kinetics of TCP in the presence of the employed scavengers. The corresponding kinetic parameters as well as the reduction of rate constants in scavenging experiments have been compiled in Table 1. i-PrOH ( $\text{HO}^\bullet$  scavenger,  $k_{\text{HO}^\bullet} = 1.9 \times 10^9$ ), methanol ( $\text{h}^+$  and  $\text{HO}^\bullet$  scavenger,  $k_{\text{HO}^\bullet} = 9.7 \times 10^8$ ),  $\text{I}^-$  ( $\text{h}^+$  and  $\text{HO}^\bullet$

**Table 1**

Kinetic Parameters (Rate constants, correlation coefficients ( $R^2$ ), Half-Life ( $t_{1/2}$ )) of TCPF in the presence of scavengers ( $[TCPF]_0 = 100 \mu\text{g L}^{-1}$ ,  $[\text{TiO}_2] = 50 \text{ mg L}^{-1}$ ,  $I = 250 \text{ W m}^{-2}$ ).

Treatment system	$k \times 10^{-2} \text{ (min)}$	$t_{1/2} \text{ (min)}$	$R^2$	% $\Delta k$
Control	5.11	13.6	0.9982	–
i-PrOH	0.32	216.6	0.9419	93.74
MeOH	0.2	346.5	0.966	96.08
NaF	3.47	20.0	0.9756	32.1
p-BQ	1.5	46.2	0.9175	70.6
ACN	0.38	182.4	0.8691	92.56
$\text{I}^-$	0.33	210.0	0.9427	93.54
Cr (VI)	4.03	17.2	0.9882	21.13
$\text{I}^- + \text{i-PrOH} + \text{N}_2$	0.14	495.0	0.9903	97.26
$\text{N}_3^-$	0.6	115.5	0.9291	88.30

scavenger,  $k_{\text{HO}^\bullet} = 1.1 \times 10^{10}$  [27] ions and MeCN as reaction media were used to discern the participation of holes and  $\text{HO}^\bullet$  in the reaction mechanism. Iodide ion is strongly bound to the  $\text{TiO}_2$  surface and has been used to estimate the quantum yield of photogenerated holes [37] while it scavenges also efficiently the resulted  $\text{HO}^\bullet_{\text{ads}}$  radicals. The rate constant decreased by 93.74%, 96.08% and 93.54% when i-PrOH, methanol and  $\text{I}^-$  ions were added to the photocatalytic system, respectively. An inhibition of 92.56% was observed when TCPF photocatalytic degradation was performed in MeCN solution. In the presence of NaF a rate constant equal to  $3.47 \times 10^{-2} \text{ min}^{-1}$  was obtained, decreasing by 32.1%, due to the transformation of  $\text{HO}^\bullet_{\text{ads}}$  to  $\text{HO}^\bullet_{\text{bulk}}$  [38]. Based on the above results, the degradation of TCPF can be proposed to take place at the surface or at least in the intimate proximity of the  $\text{TiO}_2$  particles whereas the participation of  $\text{HO}^\bullet$  in bulk water can be assumed minor. The above results clearly show the major contribution of  $\text{HO}^\bullet$  to TCPF degradation, the indirect participation of holes for the generation of  $\text{HO}^\bullet_{\text{ads}}$  and the limited direct reaction of holes (about 6–7%) with TCPF.

A reduction in the rate constant of TCPF degradation of 88.30% was observed with azide addition, a well-documented  $^1\text{O}_2$  and  $\text{HO}^\bullet$  scavenger ( $k_{^1\text{O}_2} = 4 \times 10^8 \text{ M}^{-1} \text{ s}^{-1}$ ;  $k_{\text{HO}^\bullet} = 1.2 \times 10^{10}$ ), indicating negligible participation of  $^1\text{O}_2$  in degradation mechanism. A rate constant of  $1.5 \times 10^{-2} \text{ min}^{-1}$  corresponding to 70.6% decrease of rate constant was observed with the addition of p-BQ ( $\text{O}_2 \rightarrow \cdot$  and  $\text{HO}^\bullet$  scavenger,  $k_{\text{O}_2 \rightarrow \cdot} = 1.0 \times 10^9$ ;  $k_{\text{HO}^\bullet} = 1.2 \times 10^9$ ) [27,39], proving a partial contribution of  $\text{O}_2 \rightarrow \cdot$  to TCPF degradation.

$\text{K}_2\text{Cr}_2\text{O}_7$  was used to trap  $\text{e}^-_{\text{aq}}$  produced at  $\text{TiO}_2$  conduction band leading to a slight decrease of the rate constant to  $4.03 \times 10^{-2} \text{ min}^{-1}$ . For the elucidation of direct or indirect contribution of  $\text{e}^-_{\text{aq}}$ , experiments in aqueous TCPF solution with  $\text{I}^-$  ions, i-PrOH and  $\text{N}_2$  gas flow were conducted in order to exclude all other species except reductive  $\text{e}^-_{\text{aq}}$ . Experimental results showed that the direct participation of  $\text{e}^-_{\text{aq}}$  was limited (about 3%) as a rate constant equal to  $0.14 \times 10^{-2} \text{ min}^{-1}$  was obtained. These results are in agreement with the inhibition effect observed with the addition of p-BQ, proving the indirect contribution of  $\text{e}^-_{\text{aq}}$  to form  $\text{O}_2 \rightarrow \cdot$  after the effective capturing by oxygen ( $k = 1.9 \times 10^{10} \text{ M}^{-1} \text{ s}^{-1}$ ). It is well established that  $\text{e}^-_{\text{aq}}$  can react with  $\text{O}_2$  an electron acceptor adsorbed on catalysts surface or dissolved in water, reducing it to  $\text{O}_2 \rightarrow \cdot$  [1,2].

#### 3.4. Identification of major transformation products by UPLC-TOF-MS and catalyst reuse

The screening of the photocatalytically treated samples in UW in positive (+) ESI mode allowed the identification of five TPs with a high degree of certainty (mass error < 2.2 ppm). The presence of the characteristic isotopic chlorine pattern in the mass spectrum of TPs facilitated their identification, as well. Table 2 summarizes

**Table 2**

LC-MS-TOF retention times, high resolution accurate mass data ( $[\text{M} + \text{H}]^+$ ), molecular formulas and relative error  $\Delta$  (ppm) for TCPF and the identified transformation products.

Rt (min)	TPs code	Molecular formula	$[\text{M} + \text{H}]^+$	$\Delta$ (ppm)
8.1	TCPF	$\text{C}_9\text{H}_{19}\text{Cl}_3\text{O}_4\text{P}$	327.0083	–0.6
7.5	TP343	$\text{C}_9\text{H}_{19}\text{Cl}_3\text{O}_5\text{P}$	343.0029	0.3
7.3	TP307	$\text{C}_9\text{H}_{18}\text{Cl}_2\text{O}_5\text{P}$	307.0270	–2.2
7.1	TP211	$\text{C}_8\text{H}_{20}\text{O}_4\text{P}$	211.1092	0.8
6.8	TP323	$\text{C}_9\text{H}_{18}\text{Cl}_2\text{O}_6\text{P}$	323.0213	0
6.7	TP251	$\text{C}_6\text{H}_{14}\text{Cl}_2\text{O}_4\text{P}$	250.9996	2.2

the proposed elemental composition and the exact mass values of the major TPs identified during the degradation of TCPF. In Fig. 4, UPLC-ESI-MS chromatographic profiles after 30 min of photocatalytic treatment for full scan and scan filtered  $m/z$  ions are depicted.

The TCPF molecule ( $m/z$   $[\text{M} + \text{H}]^+ = 327.0083$ ,  $\text{C}_9\text{H}_{19}\text{Cl}_3\text{O}_4\text{P}^+$ ) is an aliphatic chlorinated organophosphate compound and the results clearly demonstrated that the main structural alterations took place in the chlorinated isopropyl moieties.  $\text{HO}^\bullet$  attack at one  $-\text{CH}_3$  group of isopropyl chain resulted in the formation of hydroxylated derivative with  $m/z$   $[\text{M} + \text{H}]^+ = 343.0029$  (TP 343) and molecular formula  $\text{C}_9\text{H}_{19}\text{Cl}_3\text{O}_5\text{P}^+$ . The formation of TP307 with  $[\text{M} + \text{H}]^+$  at  $m/z$  307.0270 can be explained by the loss of one Cl atom from TCPF molecule followed by the oxidation of  $-\text{CH}_3$  group. The formation of TP323 ( $[\text{M} + \text{H}]^+ = 323.0213$ ) indicates the cleavage of one Cl atom and the simultaneous hydroxylation and oxidation of TCPF molecule and can be formed from either TP307 or TP 343.

Previous research on the reaction of hydroxyl radicals with tri-alkyl phosphates has highlighted the preferential H-abstraction at the  $\alpha$ -position relative to the phosphate functions [40,41]. Based on the effect of chlorine substitution for the reaction of chloroalkanes with  $\text{HO}^\bullet$  radicals [42] the chlorine substitution in the alkyl groups of TCPF has two different effects: (a) an inductive which decreases the reactivity for H-atom abstraction at least extending to the  $\beta$  carbon relative to the chlorine position and (b) a mesomeric effect increasing the reactivity at the  $\alpha$  carbon relative to the chlorine position with the first case to be the dominant effect [42]. Watts and Linden [28] studied the advanced oxidation (UV/ $\text{H}_2\text{O}_2$  and  $\text{O}_3/\text{H}_2\text{O}_2$ ) kinetics of four different alkyl-phosphates namely tris-2-chloroethyl phosphate (TCEP), tris-2-butoxyethyl phosphate (TBEP), tributyl phosphate (TBP) and TCPF. They have concluded that the addition of a Cl atom on the alkyl chain (e.g. TCEP) significantly reduces H-atom availability relative to TBP and TBEP and the phosphate with the chain structure having the most carbons (TBEP) had the fastest rate of reaction. However, TCPF with one more carbon on each chain than TCEP, scavenged  $\text{HO}^\bullet$  at a slower rate, most likely due to the influence of the alkyl branched chain of TCPF [28].

The H-abstraction is followed by  $\text{O}_2$  trapping resulting in the formation of peroxy-radicals that recombines giving rise to hydroxy- [43] and keto derivatives [44] or in another mechanism the generated hydroperoxide intermediate dehydrates to the corresponding aldehyde or ketone derivatives [45]. Finally, H-abstraction and the resulting carbon-centered radicals could be also followed by the addition of water leading to the formation of hydroxy-derivative according to the reaction pathways proposed for the isopropyl-function photocatalytic degradation [45].

The loss of one chloro-isopropyl group leads to the formation of TP251 ( $[\text{M} + \text{H}]^+ = 250.9996$ ,  $\text{C}_6\text{H}_{14}\text{Cl}_2\text{O}_4\text{P}^+$ ). One potential mechanism for the formation of TP251 is the direct dealkylation of the phosphate triester to the corresponding di-ester could be assigned to an addition of  $\text{HO}^\bullet$  radical to the phosphorus center and the subsequent elimination of the alkoxide radical [43,46]. In an alternative mechanism, acid catalyzed hydrolysis of the phosphate ester through the addition of photogenerated  $\text{H}^+$  to the  $\text{P}=\text{O}$  bond could be also proposed [43]. Finally, a less probable pathway via grad-

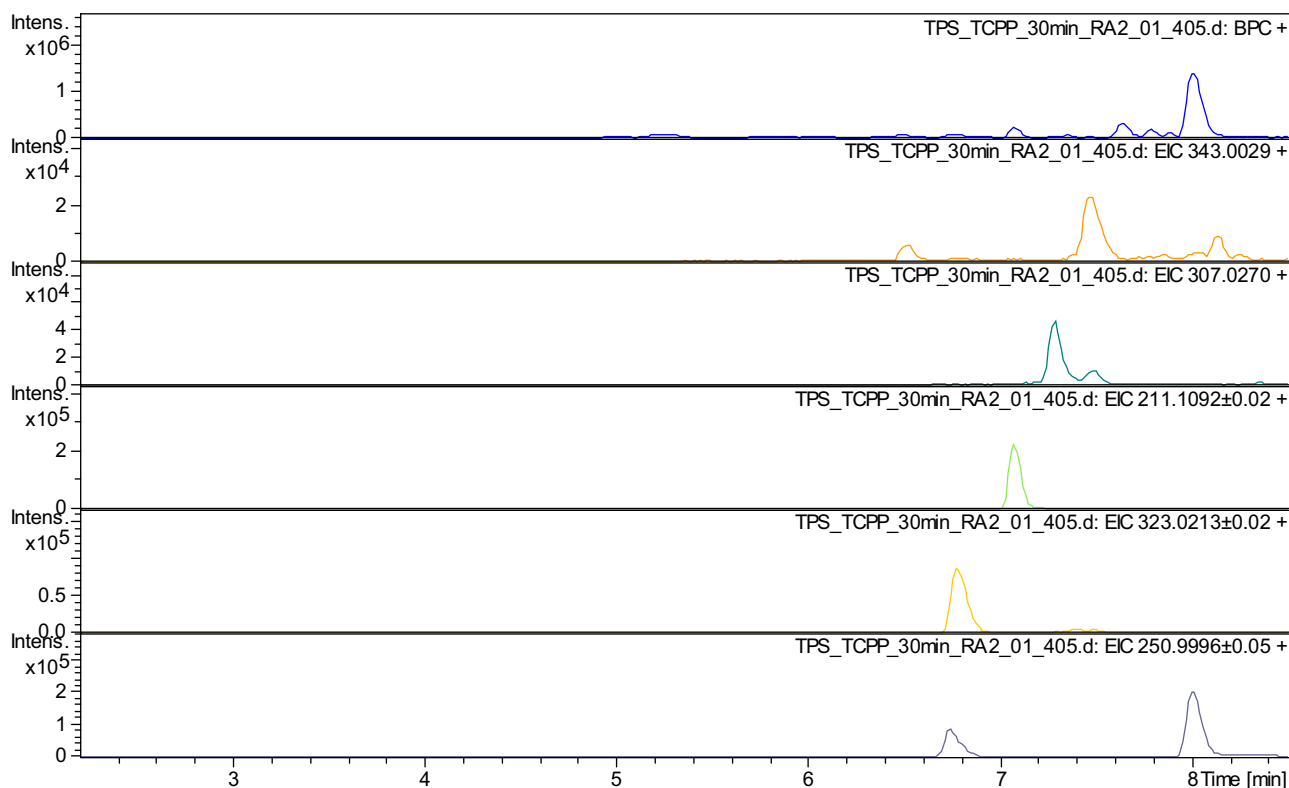


Fig. 4. UPLC-ESI-MS chromatographic profiles after 30 min photocatalytic treatment for full scan and scan filtered  $m/z$  ions.

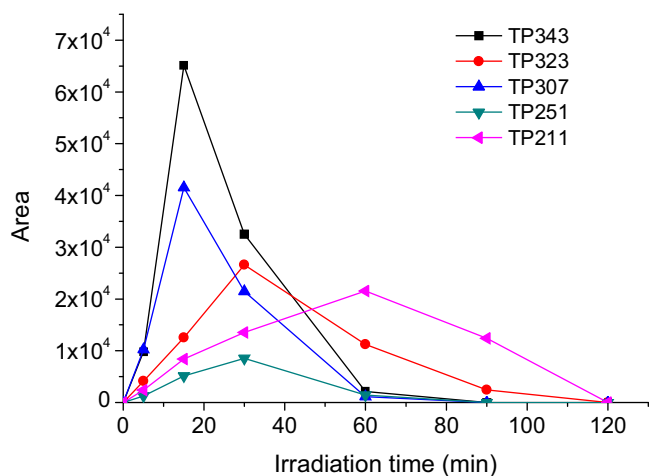


Fig. 5. Evolution profiles of identified TPs ( $[TCPP] = 100 \mu\text{g L}^{-1}$ ,  $[\text{TiO}_2] = 50 \text{ mg L}^{-1}$ ,  $I = 250 \text{ W m}^{-2}$ ).

ual demethylation by oxidation and decarboxylation reactions [47] could be also proposed.

A dechlorination reaction pathway can be proposed for the formation of TP211 ( $[M+H]^+ = 211.1092$ ,  $\text{C}_8\text{H}_{20}\text{O}_4\text{P}^+$ ) exhibited the absence of chlorine isotopic pattern in the mass spectra. A reductive dechlorination by superoxide radical ions could be proposed based on previous results dealing with the photocatalytic degradation of chlorinated aliphatic compounds [48], pentachlorophenol [49] and halogenated disinfection by-products [50]. In contrast, reductive dechlorination by  $e^-$  is supposed to be a minor pathway.

Due to the lack of analytical standards of the identified TPs, an accurate determination of the exact concentrations was not possible, thus the relative area of TPs versus irradiation time was followed. As depicted in Fig. 5, TP343 and TP307 attained its maxi-

mum area in the first stages of the process (15 min) and gradually decreased their abundance until the end of the photocatalytic treatment. TP323 and TP251 can be considered as secondary transformation products as they peak up at 30 min, following after a progressively decay. Finally, the formation of TP211 is likely a slower pathway reaching its maximum area at 60 min. At 120 min, all TPs were completely abated.

The identified TPs and their profiles are in agreement with the slow release of  $\text{PO}_4^{3-}$ , proving the preservation of phosphate core of TCPP molecule till more prolonged irradiation times. On the other hand, more rapid release of  $\text{Cl}^-$  is proved once more by the identification of dechlorinated TPs. Combining the above results on the identified TPs and their evolution profiles as well as the evolution of ions release the degradation could be considered to proceed through hydroxylation, oxidation, dealkylation and dechlorination pathways and a proposed degradation mechanism is given in Fig. 6.

Taking into account the aliphatic structure of TCPP and the results obtained in the present study, as final TPs, compounds such as the methyl esters of phosphoric acid, formic, acetic, glycolic, oxalic acids and phosphates can be considered [18,51]. A great effort was also devoted to elucidate TPs generated during the photocatalytic removal of TCPP using wastewater as matrix. In this case, only TP307 and TP251 have been identified. Both TPs emerged at prolonged treatment times (120 min) and remained abundant in the reaction solution until 360 min showing once more the notable effect of water matrix composition on the photocatalytic process.

Since the stability and recyclability of photocatalysts are of great importance for industrial applications, the photocatalytic degradation of TCPP for three consecutive cycles was investigated and the kinetics profiles are presented in Fig. 7. TCPP removal after 60 min of irradiation decreased only about 10% probably due to the accumulation of end-product in the surface of the catalyst. The observed loss of efficiency is similar with that reported in other studies for

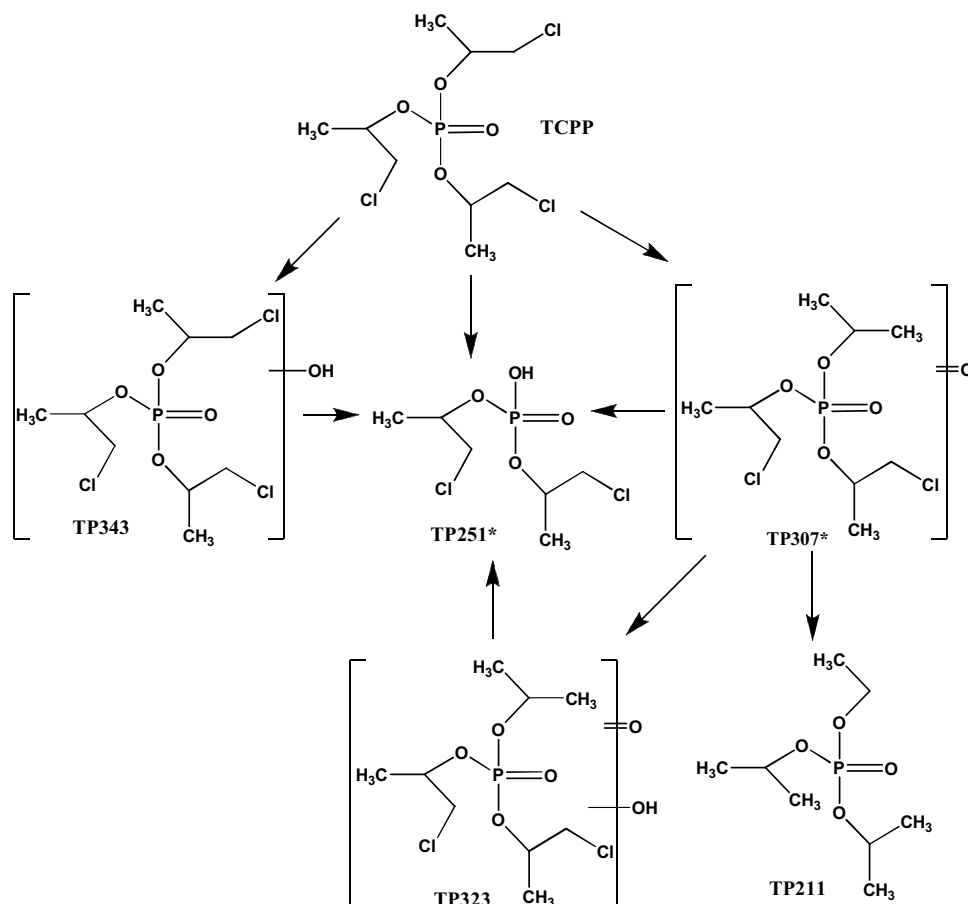


Fig. 6. Proposed degradation pathways of TCPP photocatalytic degradation in the presence of  $\text{TiO}_2$  and simulated solar light in UW (\*TPs identified in WW, as well).

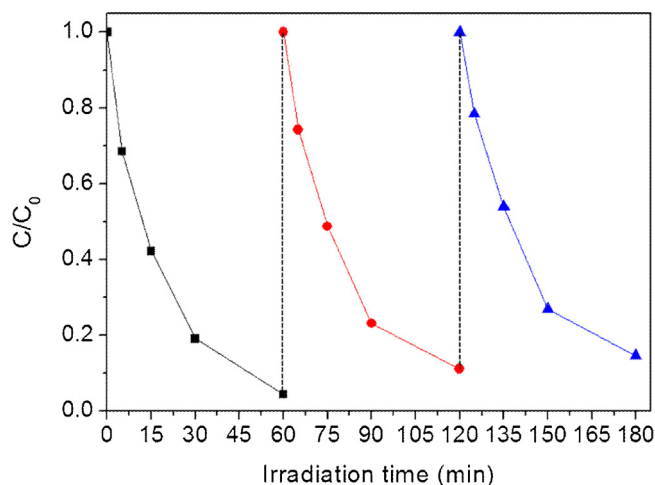


Fig. 7. Photocatalytic degradation profiles of TCPP after three consecutive catalytic cycles ([TCPP] =  $100 \mu\text{g L}^{-1}$ ,  $[\text{TiO}_2]$  =  $50 \text{ mg L}^{-1}$ ,  $I$  =  $250 \text{ W m}^{-2}$ ).

the use of  $\text{TiO}_2$  P25 in three catalytic cycles for the degradation of dyes and phenol [52,53].

### 3.5. Ecotoxicity assessment

For the complete evaluation of treatment technologies, the ecotoxicological tests are considered to be useful tools. The evolution of toxicity during the photocatalytic treatment was monitored using *Vibrio Fischeri* assay in order to provide further evaluation of the

applied process in both matrices. Photocatalytically treated samples at different treatment stages were analyzed to estimate the percentage of inhibition of each sample after various exposure times i.e. 5, 15, 30, 60 and 90 min. An increase in the inhibitory effect was observed up to 30 min of exposure, reaching a plateau thereafter, thus Fig. 8a depicts the data measured after 30 min of incubation in UW. The initial solution of TCPP showed an inhibitory percentage of 21%. With the progressively abatement of TCPP, the percentage inhibition decreases and after 240 min the toxicity reaches a final value of less than 2%. This trend indicates that TCPP degradation proceeds with the formation of less toxic TPs compared to the parent compound. The lower toxicity can be attributed to the dechlorinated and more polar generated TPs [54].

Fig. 8b illustrates the evolution of inhibition as a function of photocatalytic treatment using WW as matrix. As shown in Fig. 6b, the inhibition of the untreated solution of TCPP (WW spiked with  $100 \mu\text{g L}^{-1}$  TCPP) is 47% that is slightly increased to 55% after 30 min of irradiation. After that time, inhibition percentages decrease slowly and only after prolonged irradiation time low toxicity, less than 14%, was achieved. The results indicate that the initial toxicity of the solution originates partially, from compounds present in wastewater. This was verified by the initial toxicity of the wastewater sample which showed an inhibition of 23%. Moreover near additive effects between TCPP and organic and inorganic compounds present in the wastewater was indicated. The slight increase in 30 min can be attributed to the by-products of wastewater's organic content formed during the photocatalytic treatment. Similarly to our results, an increase in the toxicity during the first stages has also been observed during the treatment of wastewater with phenolic content by different AOPs [7,55]. Toxicity decrease

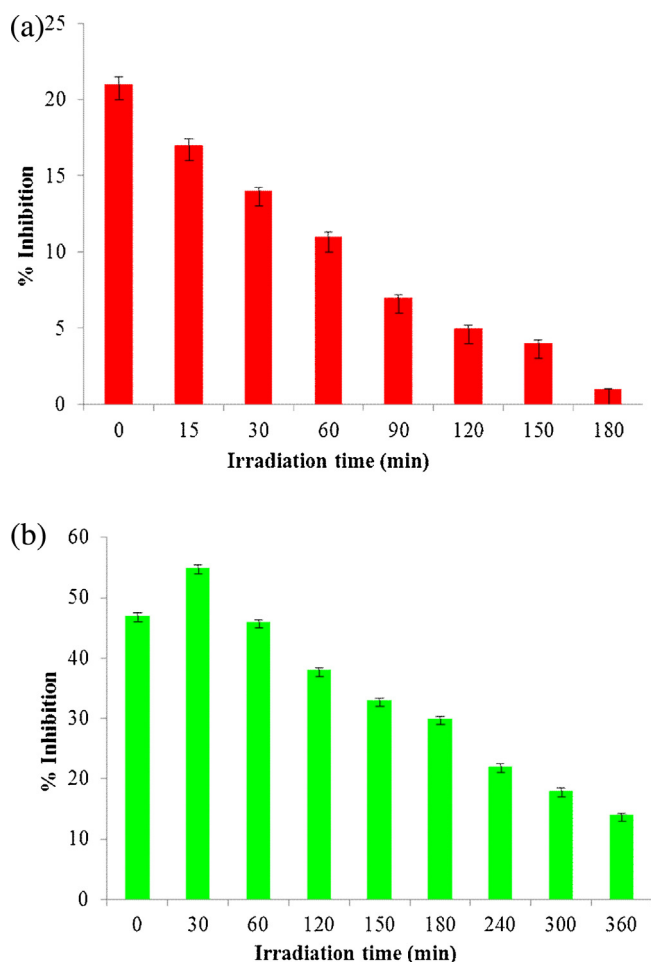


**Fig. 8.** Inhibition (%) of the luminescence of bacteria *Vibrio Fischeri* as a function of the photocatalytic treatment in (a) UW, (b) WW ([TCPP] = 100  $\mu\text{g L}^{-1}$ ,  $[\text{TiO}_2]$  = 50  $\text{mg L}^{-1}$ ,  $I$  = 250  $\text{W m}^{-2}$ ).

with the progression of the treatment is in agreement with the total phenols' removal and reduction of aromatic content described previously.

#### 4. Conclusions

In recognition of the lack of data regarding the removal of flame retardants pollutants by advanced oxidation technologies, the degradation of TCPP by heterogeneous photocatalysis is presented for first time. This work is the first one revealing comprehensive data regarding the photocatalytic degradation of TCPP in UW and WW, the identification of the main TPs and finally the assessment of toxicity evolution during the process. A major issue that has been taken into serious consideration is related with the utilization of realistic conditions i.e. concentration of TCPP in  $\mu\text{g L}^{-1}$  as well as simulated solar light at room temperature and atmospheric pressure under the framework of green chemistry. The findings arrived from the overall assessment of heterogeneous photocatalysis to remove TCPP under realistic conditions suggest that the degradation is mainly carried out by  $\text{HO}^\bullet$  radical attack and hindered significantly in wastewater due to organic matter and inorganic ions quenching. UPLC-TOF-MS analyses showed that the main TCPP transformation pathways were hydroxylation and oxidation followed by dechlorination and dealkylation reactions. The toxicity of treated solutions gradually decreased due to the subsequent degradation of TPs.

#### Acknowledgments

This research has been co-financed by the European Union (European Social Fund – ESF) and Greek national funds through the Operational Program “Education and Lifelong Learning” of the National Strategic Reference Framework (NSRF)—Research Funding Program: THALIS (MIS:379409). Investing in knowledge society through the European Social Fund.

#### Appendix A. Supplementary data

Supplementary data associated with this article can be found, in the online version, at <http://dx.doi.org/10.1016/j.apcatb.2016.03.039>.

#### References

- [1] I.K. Konstantinou, T.A. Albanis, Appl. Catal. B: Environ. 42 (2003) 319–335.
- [2] I.K. Konstantinou, T.A. Albanis, Appl. Catal. B: Environ. 49 (1) (2004) 1–14.
- [3] M. Pelaez, N.T. Nolan, S.C. Pillai, M.K. Seery, P. Falaras, A.G. Kontos, P.S.M. Dunlop, J.W.J. Hamilton, J.W. Byrne, K. O'shea, M.H. Entezari, D.D. Dionysiou, Appl. Catal. B: Environ. 125 (2012) 331–349.
- [4] A. Amine-Khodja, A. Boulkamh, C. Richard, Appl. Catal. B: Environ. 59 (2005) 147–154.
- [5] M. Antonopoulou, A. Giannakas, Y. Deligiannakis, I. Konstantinou, Chem. Eng. J. 231 (2013) 314–325.
- [6] Y. Lin, C. Ferronato, N. Deng, F. Wu, J.M. Chovelon, Appl. Catal. B: Environ. 88 (2009) 32–41.
- [7] M. Antonopoulou, V. Papadopoulos, I. Konstantinou, J. Chem. Technol. Biotech. 87 (2012) 1385–1395.
- [8] M. Farré, S. Pérez, L. Kantiani, D. Barceló, Trends Anal. Chem. 27 (11) (2008) 991–1007.
- [9] E.D. Schreder, M.J. La Guardia, Environ. Sci. Technol. 48 (2014) 11575–11583.
- [10] A. Marklund, B. Andersson, P. Haglund, Environ. Sci. Technol. 39 (19) (2005) 7423–7429.
- [11] J. Regnery, W. Püttman, Water Res. 44 (2010) 4097–4104.
- [12] J. Andresen, A. Grandmann, K. Bester, Sci. Total Environ. 332 (2004) 155–166.
- [13] H. Fang, Y. Gao, G. Li, J. An, P.K. Wong, H. Fu, S. Yao, X. Nie, T. An, Environ. Sci. Technol. 47 (2013) 2704–2712.
- [14] R. Palominos, J. Freer, M.A. Mondaca, H.D. Mansilla, J. Photochem. Photobiol. A 193 (2008) 139–145.
- [15] S. Parvez, C. Venkataraman, S. Mukherji, Environ. Int. 32 (2006) 265–268.
- [16] M. Fathinia, A.R. Khataee, M. Zarei, S. Aber, J. Mol. Catal. A: Chem. 333 (1–2) (2010) 73–84.
- [17] M. Sleiman, D. Vildozo, C. Ferronato, J.-M. Chovelon, Appl. Catal. B: Environ. 77 (1–2) (2007) 1–11.
- [18] T. Oncescu, M.I. Stefan, P. Oancea, Environ. Sci. Pollut. Res. 17 (2010) 1158–1166.
- [19] E. Evgenidou, I. Konstantinou, K. Fytianos, T. Albanis, J. Hazard. Mater. 137 (2006) 1056–1064.
- [20] S. Carbonaro, M.N. Sugihara, T.J. Strathmann, Appl. Catal. B: Environ. 129 (2013) 1–12.
- [21] W. Zhang, Y. Li, Y. Su, K. Mao, Q. Wang, J. Hazard. Mater. 215–216 (2012) 252–258.
- [22] N. Rioja, S. Zorita, F.J. Peñas, Appl. Catal. B: Environ. 180 (2016) 330–335.
- [23] J.E. Donham, E.J. Rosenfeldt, K.R. Wigginton, Environ. Sci. Process Impacts 16 (2014) 764–769.
- [24] C. Postigo, C. Sirtori, I. Oller, S. Malato, M.I. Maldonado, M. López de Alda, D. Barceló, Appl. Catal. B: Environ. 104 (2011) 37–48.
- [25] P. Karaolia, I. Michael, I. García-Fernández, A. Agüera, S. Malato, P. Fernández-Ibáñez, D. Fatta-Kassinos, Sci. Total Environ. 468–469 (2014) 19–27.
- [26] B.-L. Yuan, X.-z. Li, N. Graham, Chemosphere 72 (2008) 197–204.
- [27] G.V. Buxton, C.L. Greenstock, W.P. Helman, A.B. Ross, J. Phys. Chem. Ref. Data 17 (1988) 513–886.
- [28] M.J. Watts, K.G. Linden, Environ. Sci. Technol. 43 (2009) 2937–2942.
- [29] S. Ahmed, M.G. Rasul, R. Brown, M.A. Hashib, J. Environ. Manage. 92 (2011) 311–330.
- [30] N.M. Mahmoodi, M. Armani, N.Y. Lymaee, K. Gharanjig, J. Hazard. Mater. 145 (2007) 65–71.
- [31] R. Wu, C. Chena, M. Chen, C. Lu, J. Hazard. Mater. 162 (2009) 945–953.
- [32] P. Neta, R.E. Huie, A.B. Ross, J. Phys. Chem. Ref. Data 17 (1988) 1027–1284.
- [33] D.E. Santiago, J. Arána, O. González-Díaz, M.E. Alemán-Domínguez, A.C. Acosta-Dacal, C. Fernandez-Rodríguez, J. Pérez-Peña, J.M. Doña-Rodríguez, Appl. Catal. B: Environ. 156–157 (2014) 284–292.
- [34] C. Guillard, E. Puzenat, H. Lachheb, A. Houas, J.M. Hermann, Int. J. Photoenergy 7 (2007) (10.1155).
- [35] R.A. Burns, J.C. Crittenden, D.W. Hand, V.H. Selzer, L.L. Sutter, S.R. Salaman, J. Environ. Eng. 125 (1999) 77–85.
- [36] J. Mack, J.R. Bolton, J. Photochem. Photobiol. A: Chem. 128 (1999) 1–13.

- [37] K.I. Ishibashi, A. Fujishima, T. Watanabe, K. Hashimoto, J. Photochem. Photobiol. A: Chem. 134 (2000) 139–142.
- [38] C. Minero, G. Mariella, V. Maurino, D. Vione, E. Pelizzetti, Langmuir 16 (2000) 8964–8972.
- [39] B.H.J. Bielski, D.E. Cabelli, R.L. Arudi, A.B. Ross, J. Phys. Chem. Ref. Data 14 (1985) 1041–1100.
- [40] M.N. Schuchmann, M.L. Scholes, H. Zegota, C. von Sonntag, Int. J. Radiat. Biol. 68 (1995) 121–131.
- [41] G.I. Khaikin, High Energy Chem. 32 (1998) 287–289.
- [42] F. Markert, O.J. Nielsen, Chem. Phys. Lett. 194 (1992) 123–127.
- [43] Y.C. Oh, Y. Bao, W.S. Jenks, J. Photochem. Photobiol. A: Chem. 161 (2003) 69–77.
- [44] G.A. Russell, J. Am. Chem. Soc. 79 (1957) 3871–3877.
- [45] E. Pelizzetti, C. Minero, V. Carlin, M. Vincenti, E. Pramauro, M. Dolci, Chemosphere 24 (1992) 891–910.
- [46] K.E. O'Shea, S. Beightol, I. Garcia, M. Aguilar, D.V. Kalen, W.J. Cooper, J. Photochem. Photobiol. A: Chem. 107 (1997) 221–226.
- [47] M.V. Phanikrishna Sharma, V. Durga Kumari, M. Subrahmanyam, Chemosphere 72 (2008) 644–651.
- [48] H. Che, W. Lee, Chemosphere 82 (2011) 1103–1108.
- [49] Y. Li, J. Niu, L. Yin, W. Wang, Y. Bao, J. Chen, Y. Duan, J. Environ. Sci. 23 (2011) 1911–1918.
- [50] D. Gerrity, B. Mayer, H. Ryu, J. Crittenden, M. Abbaszadegan, Water Res. 43 (2009) 1597–1610.
- [51] G.R.M. Echavía, F. Matzusawa, N. Negish, Chemosphere 76 (2009) 595–600.
- [52] E.M. Saggioro, A.S. Oliveira, T. Pavesi, C. Gil Maia, L.F. Vieira Ferreira, J. Costa Moreira, Molecules 16 (2011) 10370–10386.
- [53] S. Mozia, P. Brozek, J. Przepiórski, B. Tryba, A.W. Morawski, J. Nanomat. (2012), Article ID 949764.
- [54] Q.T. Liu, T.D. William, R.I. Cumming, G. Holm, M.J. Hetheridge, R. Murray-Smith, Environ. Toxic. Chem. 28 (2009) 2622–2631.
- [55] R.C. Martins, A.F. Rossi, R.M. Quinta-Ferreira, J. Hazard. Mater. 180 (2010) 716–721.